Experiments with planar inductive ion source meant for creation of H^+ beams

J. H. Vainionpää, T. Kalvas, S. K. Hahto[20], J. Reijonen

Lawrence Berkeley National Laboratory, 1 Cyclotron Rd, Berkeley, CA 94720, USA

PACS:29.25.Ni, 52.50.Dg, 52.75.-d

Keywords: Ion sources, External rf-antenna, plasma source, planar inductive source

(Received:

Abstract: In this article the effect of different engineering parameters of an rf-driven ion sources with external spiral antenna and quartz disk rf-window are studied. Paper consists of three main topics: The effect of source geometry on the operation gas pressure, the effect of source materials and magnetic confinement on extracted current density and ion species and the effect of different antenna geometries on the extracted current density. The operation gas pressure as a function of the plasma chamber diameter, was studied. This was done with three cylindrical plasma chambers with different inner diameters. The chamber materials were studied using two materials, aluminum and alumina (AlO_2). The removable 14 magnet multicusp confinement arrangement enabled us to compare the effects of the two wall materials with and without the magnetic confinement. Highest proton fraction of $\approx$ 87 % at 2000 W of rf-power and at pressure of 1.3 Pa was measured using AlO_2 plasma chamber and no multicusp confinement. For all the compared ion sources at 1000W of rf-power, source with multicusp confinement and AlO_2 plasma chamber yields highest current density of 82.7 mA/cm^2 at operation pressure of 4 Pa. From the same source highest measured current density of 143 mA/cm^2 at 1.3 Pa and 2200W of rf-power was achieved. Multicusp confinement incrased the maximun extracted current up to factor of two. Plasma production with different antenna geometries was also studied. Antenna tests were performed using same source geometry as in source material study with AlO_2 plasma chamber and multicusp confinement. The highest current density was achieved with 4.5 loop solenoid antenna with 6 cm diameter. Slightly lower current density with lower pressure was achieved using tightly wound 3 loop spiral antenna with 3.3 cm ID and 6 cm OD.

I. Introduction

Plasma sources with low operation gas pressure and high intensity with good atomic hydrogen species are required in various applications, including cyclotron injection and neutron generators. In many cases problems arise from the high voltage stability as high voltage section of the generator is in too high pressure. Applications with large extraction apertures and/or limited or non-existent pumping, require ion sources with low operation pressure.[1–4]

The two ion sources in this article are developed for driver for the neutral beam injection in Princenton Plasma Physics Laboratory (PPPL) (see figure 2) and driver for portable neutron generator for Adelphi Technologies Inc. (see figure 3). In the PPPL source extraction aperture is very large $\approx$40 cm^2 and in the Adelphi source pumping is limited. Thus both sources need to operate in low operation pressures and still produce intensive ion beams, in addition PPPL source also needs to have homogeneous plasma in the large extraction area and create beam with a good atomic fraction. Similar planar sources that is presented in figure 2 are used as a deposition and implantation plasma sources[5–7] and are shown to produce homogeneous plasma with low pressures. In preliminary tests of PPPL source it was noted that the source is capable of producing dense and homogeneous plasma at low pressures (0.2–1 Pa). Due to low operation pressures similar design to the PPPL source was also selected for the Adelphi source. In this article we present the measurement results for the dependence of operation pressure from size of the source, the effect of source materials and magnetic confinement on extracted current density and ion species and the effect of different antenna geometries on the extracted current density.

Motivation for publishing our measurement results in this article was absence

of these kind of measurements in the literature. For the material measurements there are some theoretical and experimental studies[8 – 12] about effect of liners and source materials to the plasma parameters but we did not found measured data concerning planar inductive ion source operated with hydrogen or deuterium gas.

II. Beam extraction and diagnostics

In figure 1 a schematic of the extraction and the beam diagnostics setup used in the following measurements is shown. To measure currents independent of plasma meniscus geometry and space charge effects, all of the current measurements of this article are ion saturation currents and thus independent of extraction voltage. Ion currents were measured using movable Faraday cup FC1 with electrostatic secondary electron suppression. The species extracted from the ion source was measured using magnetic analyzer, that separates particles with different charge/mass ratio. All the diagnostics were made using a computerized measurement setup shown in the figure 1. The beam extraction is simple two electrode diode arrangement with 2 mm extraction gap. Extraction aperture of 2 mm was used.

III. Ion sources

Figures 2 and 3 show schematic of the ion sources used in the experiments. Design of the ion source A was made so that cylindrical chamber wall would be easy to change and cusp magnets were easy to add or remove. Ion source A was used to test the effects of the plasma confinement and the chamber wall materials to

the measured species and saturation current densities. Back flange of the cylindrical source was for an insulator window and rf-antenna and the other end of the source was for extraction and for the gas feed-troughs. Source A was also used to measure the current densities with different antenna geometries. In type B ion source extraction aperture and gas feed-troughs were located in cylinder wall and ends of the cylinder were for rf insulator window and antenna. To test the effects of chamber size to minimum and optimum operation pressure, three type B ion sources with different chamber diameter D were built. For all measurements the ion sources were driven with 12.56 MHz rf-power supply which was matched to antenna using step down transformer matching network.[13] The operation pressures of the source was measured using capacitive pressure meter.

IV. Plasma chamber geometries

Collisions between fast electrons and neutrals is required to form a plasma.[14,15,16] For sources under study, primary electrons (electrons accelerated by rf antenna) accelerated by induction fields, travel approximately parallel to the insulator window surface.[17] By increasing the average time of flight for primary electrons (diameter of the source) we can decrease the operation gas pressure and the collision frequency between electrons and neutrals while maintaining the amount of ionized particles. On the other hand, the plasma density decreases because the volume of the ion source increases proportional to the square of the radius and loss area in the walls is increasing linearly as a function of the radius.

We studied the effect of the plasma chamber diameter as a function of the operation pressure using sources presented in figure 3. Three different plasma

chamber diameters were used: $D_1 = 6$ cm, $D_2 = 7.5$ cm and $D_3 = 10$ cm. Estimated minimum and optimum pressure versus source diameter is plotted in figure 4. Here optimum pressure is the point where extracted current has the largest value and minimum pressure is pressure where plasma is hard to maintain because pressure is too low (dimensions of the source are same scale as electron mean free bath). For all the pressure measurements the ion sources were operated with same antenna and rf-power.

Behavior of the plot in figure 4 can be explained by changing electron temperature because mean free bath is proportional to pressure and electron energy.[14,15,16] Electron temperature and thus pressure behavior in figure 4 is affected by plasma density and the efficiency of energy transfer from primary electrons to plasma. In a denser plasma collisions of charged particles affect more to the trajectories of primary electrons. This causes energy of primary electrons to be distributed between number of electrons and thus changes cross section of ionization, number and lifetime of the energetic electrons.[8,18] Also smaller sources lose more high energy primary electron to the source walls which lowers the electron temperature. For small source, metal walls close to the antenna may also affect rf-matching and thus operation pressures.

V. Plasma chamber materials

Aluminum and alumina plasma chamber wall materials were compared and effect of the magnetic confinement was studied. Test were carried out with source type A shown in figure 2 by changing chamber wall material and removing or adding the multicusp confinement magnets. In figures 5-8 we can see effect of magnetic

confinement and source chamber material to extracted saturation current densities and the H^+ fraction. Same antenna and window material SiO_2 was used for all the measurements only rf-power or operation pressure was varied.

The current density is higher in magnetically confined source due to increase of the lifetime of the electrons. In magnetically confined plasma the optimum operation pressure and minimum operation pressure for this type of source was slightly higher than when using a source without the magnetic confinement. Behavior might be caused by multicusp field witch creates magnetic mirror that prevents some primary electrons from entering the plasma chamber.[15]

Major reactions 2–7 inside plasma are listed below.

$$\mathrm{H_2} + e_f \rightarrow \mathrm{H_2^+} + e \quad (1)$$

$$\mathrm{H_3^+} + e_f \rightarrow \mathrm{H^+}, \mathrm{H_2}/2\mathrm{H}, e \quad (2)$$

$$\mathrm{H} + e_f \rightarrow \mathrm{H^+} + 2e \quad (3)$$

$$\mathrm{H_2^+} + \mathrm{H_2} \rightarrow \mathrm{H_3^+} + \mathrm{H} \quad (4)$$

$$\mathrm{H_2} + e_f \rightarrow 2\mathrm{H} + 2e \quad (5)$$

$$\mathrm{H_2^+} + e_f \rightarrow \mathrm{H}, \mathrm{H} \quad (6)$$

$$\mathrm{H_3^+} + e_f \rightarrow \mathrm{H_2}, \mathrm{H}/3\mathrm{H} \quad (7)$$

At low pressures the decrease of electron temperature could explain low H^+ fraction with multicusp confinement compared to case without the confinement. At lower electron energy reaction rates of reactions 3, 4 and 6 decrease and simultaneously reaction rates of reactions 7 and 7 increase.[18,8] At higher pressures reaction rate increase of reaction 5 would explain slight increase in H_3^+ and corresponding decrease of H^+ fraction.

It is suspected that surface chemistry plays a big role in species distribution of

the extracted beam. Chan *et.al*[8] and Takagi *et.al*[19] presented that some surfaces like quartz and hot metal wall reduces a recombination of H to H_2 and increases the dissociation of incident H_2 molecules to H. Higher H fraction in residue gas increases fractions of H^+ ions trough reaction 4. This might explain higher H^+ fraction of AlO_2 source wall compared to Al source wall. It is possible that if the chamber walls are conductive material some, of the rf-power couples to the walls instead of plasma. This may lead to different species fractions and current densities between AlO_2 and Al chambers.

In figures 7,8 we see current density and H^+ fraction plotted versus power. Increasing plasma density and amount of fast electrons at higher power causes H^+ fraction and measured saturation currents to rise. With aluminum the amount of impurities increases from $\approx 10\ \%$ to $\approx 20\ \%$ when increasing the power from 1400 W to 1600 W. For alumina amount of impurities stays the same $\approx 10\ \%$ regardless of the power. This may explain why H^+ curve of source with aluminum wall behaves so oddly in figure 8.

VI. Antenna test

Antenna tests were done by driving the plasma with four different antennas.

1. loosely wound 3.5 loop spiral antenna with 2.5 cm inner diameter (ID) and 9 cm outer diameter (OD).
2. loosely wound 2 loop spiral antenna with 6 cm ID and 9 cm OD.
3. tightly wound 3 loop spiral antenna with 3.3 cm ID and 6 cm OD.
4. 4.5 loop solenoid antenna, 6 cm diameter and 3 cm long.

The extracted current density as function of pressure is shown in figures 9. The current density as a function of pressure seems to be fairly similar for all the antenna geometries. Minor differences of current densities are a sum of few different phenomena. Efficiency of matching might be different for different antennas. For antennas with large OD the multicusp magnetic confinement fields may generate rf-coupling issues. Also diffusion of plasma from high plasma density area near the rf-antenna to the extraction area might be affected by the magnetic fields. This may explain why antenna #2 performed so poorly and antenna #3 well. Antenna #2 is located mostly at the edge of the insulator window where magnetic fields are strongest and antenna #3 in the middle at the field free region of the rf-window. Different geometry of the antenna means that geometry of the induced magnetic field is also different. Antenna geometry, which generates field geometry that penetrates most efficiently trough the insulator window to the plasma, also generates high density plasma and consequently high extracted current density.

VII. Discussion

It was shown that by increasing source diameter beyond certain point, has little effect on the minimum and the optimum operation pressures. To further decrease the operation pressures of the ion source, other means such as better magnetic confinement can be effectively used.

Comparison between Al and AlO_2 chamber wall materials suggests that using insulators as discharge chamber material increases the H^+ fraction of the extracted ions. Some tests were also made to compare AlO_2 and SiO_2 insulator window materials. Quartz as a window was chosen for two reasons: higher extracted current

densities (by up to 20 %), and the mechanical strength under high temperature operation in comparison to the alumina. In future different insulator window and source wall materials such as quartz and some ceramics like aluminum nitride and micalex could be tested. Multicusp confinement enhances the extracted currents but has little effect to H^+ fraction and minimum operation pressure. In various other sources decrease in operation pressure is detected when adding multicusp confinement. In source A placing of the multicusp magnets might create magnetic mirror effect that prevents primary electron from entering the plasma chamber thus preventing the operation pressure improvement of the multicusp confinement.

For a given ion source, solenoid antenna provides higher current densities than similar size spiral antenna. The operation pressure of the ion source is higher when operated with the solenoid antenna than with the spiral antenna. For external spiral antennas with different inner and outer diameters were compared. Antenna with large OD and ID performed poorly compared to the tightly wound small ID and OD antenna or more loosely wound large OD small ID antenna. Probably due different field geometry and diffusion of plasma to the extraction.

Acknowledgments

The author would like to thank S. B. Wilde, T. McVeigh and P. Wong for their technical support and advice and J. Kwan for the fruitful discussions. This work is supported by ADELPHI Technologies Inc., Nova Photonics Inc. and by Department of Energy under contract no. DE-AC02-05CH11231.

References

[1] X. Jiang, Y. Chen, L. Ji, Q. Ji, K. N. Leung, Rev. Sci. Instrum. **76**, 103302, (2005).

[2] J. Reijonen, K. N. Leung, G. Jones, Rev. Sci. Instrum **73**, pp. 934–936 (2002).

[3] J. Reijonen, Proceedings of 2005 Particle Accelerator Conference, Knoxville, Tennessee.

[4] J. Reijonen, F. Gicquel, S. K. Hahto, M. King, T. P. Lou, K. N. Leung, Applied Radiation and Isotopes 63 pp. 757–763 (2005).

[5] P. Chabert, H. Abada, and J.-P. Booth, J. Appl. Phys. 94. 1 (2003).

[6] E. L. Tsakadze,K. N. Ostrikov, S. Xu, J. Appl. Phys. 91. 1 (2002).

[7] O. A. Popov, *High Density Plasma Sources*, (Noyes Publications, Park Ridge, New Jersey, USA 1995) pp.76-98

[8] C. F. Chan, C. F. Burnell, William S. Cooper, J. Appl. Phys **54**, pp. 6119–6137 (1983).

[9] N. Gascon, M. Dudeck, S. Barral, Physic of plasmas. 10, 10 (2003).

[10] S. Barral, K. Makowski, and Z. Peradzynt'ski, Phys. Plasmas. 10, 10 (2003).

[11] Y. Saito, Y. Mitsuoka, and S. Suganomata Rev. Sci. Instrum. 55, 1760 (1984).

[12] Bai Gui Bin, Rev. Sci. Instrum. 61, pp. 478-480 (1990).

[13] J. Staples, T. Schenkel, Particle Accelerator Conf., Chicago, IL, pp. 2108–2110 (2001).

[14] I. C. Brown, *The Physics And Technology Of Ion Sources*, John Wiley & Sons, 1989.

[15] R. Fitzpatrick, *Introduction to Plasma Physics: A graduate course lecture notes*, The University of Texas at Austin, http://farside.ph.utexas.edu/teaching/plasma/plasma.html, 2006.

[16] T. Smid, *Theoretical Principles of Plasma Physics and Atomic Physics* http://www.plasmaphysics.org.uk/.

[17] P. Colpo, T. Meziani, F. Rossi, J. Vac. Sci. Technol. A: Vacuum, Surfaces, and Films **23**, pp. 270–277 (2005).

[18] C. F. Barnett *Atomic Data for Fusion. Volume 1: Collisions of H, H2, He, and Li Atoms and Ions with Atoms and Molecules*, ORNL-6086 (http://www-cfadc.phy.ornl.gov/redbooks/redbooks.html) (1990).

[19] T. Takagi, I. Yamada, J. Ishikawa, F. Sano, N. Kusano, Proceedings of the second symposium on ion sources and formation of ion beams, 1974; Berkeley, California, USA.

[20] Current affiliation: SemEquip, Inc. 34 Sullivan Rd, North Billerica, MA 01862, USA

Figure captions

1. Figure 1: Extraction and diagnostic setup. From extraction to FC2 beam travels about 2.5 m.

2. Figure 2: Ion source type A. Back flange of the ion source is for rf-antenna and insulator window. Water cooled confinement magnets are located against the cylindrical chamber wall. Front flange of the source is for extraction hole and gas feed-troughs.

3. Figure 3: Ion source type B. Two rf-antennas and insulator windows located at the ends of the cylindrical chamber wall. Extraction of the ion beam and gas feed-troughs are located in the sides of the cylindrical chamber wall.

4. Figure 4: Minimum and optimum pressure versus diameter measured at 1000 W of rf-power.

5. Figure 5: Extracted saturation current density plotted as a function of pressure measured at 1000 W of rf-power.

6. Figure 6: H^+ fraction plotted as a function of pressure measured at 1000 W of rf-power.

7. Figure 7: Extracted saturation ion current densities plotted as a function of power at pressure of 1.3 Pa.

8. Figure 8: H^+ fraction plotted as a function of power at pressure of 1.3 Pa.

9. Figure 9: Antenna species and current versus pressure at 1000 W of rf power.

Figures

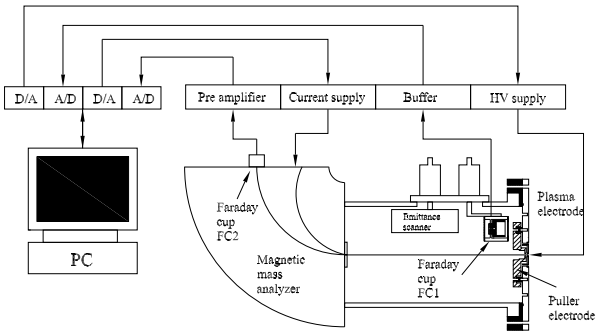

Figure 1: Extraction and diagnostic setup. From extraction to FC2 beam travels about 2.5 m.

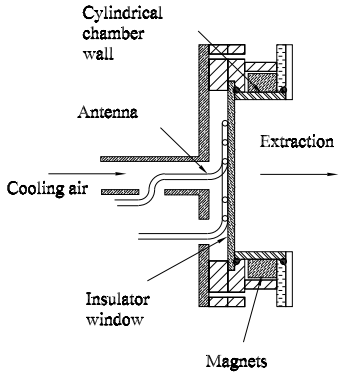

Figure 2: Ion source type A. Back flange of the ion source is for rf-antenna and insulator window. Water cooled confinement magnets are located against the cylindrical chamber wall. Front flange of the source is for extraction hole and gas feed-troughs.

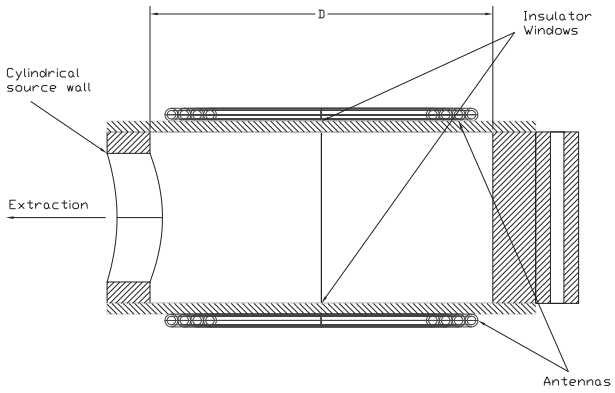

Figure 3: Ion source type B. Two rf-antennas and insulator windows located at the ends of the cylindrical chamber wall. Extraction of the ion beam and gas feed-troughs are located in the sides of the cylindrical chamber wall.

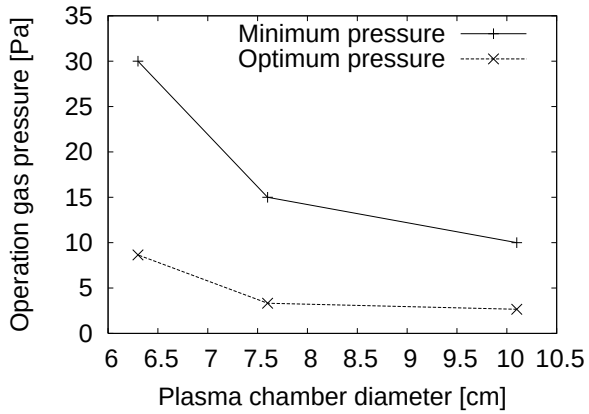

Figure 4: Minimum and optimum pressure versus diameter measured at 1000 W of rf-power.

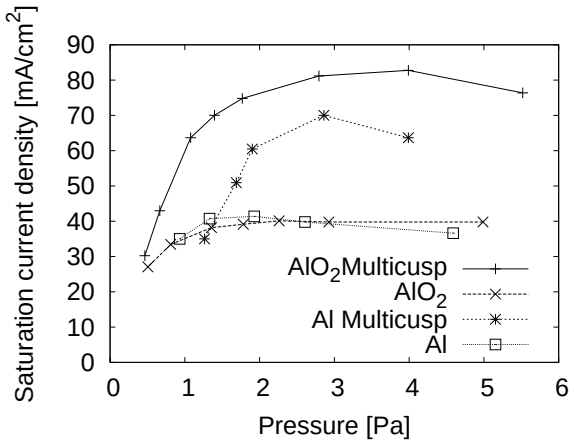

Figure 5: Extracted saturation current density plotted as a function of pressure measured at 1000 W of rf-power.

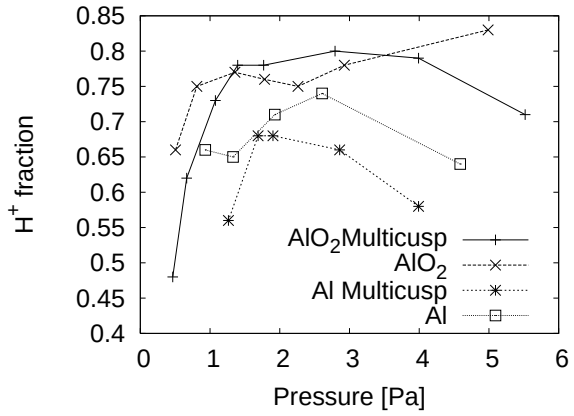

Figure 6: H_1^+ fraction plotted as a function of pressure measured at 1000 W of rf-power.

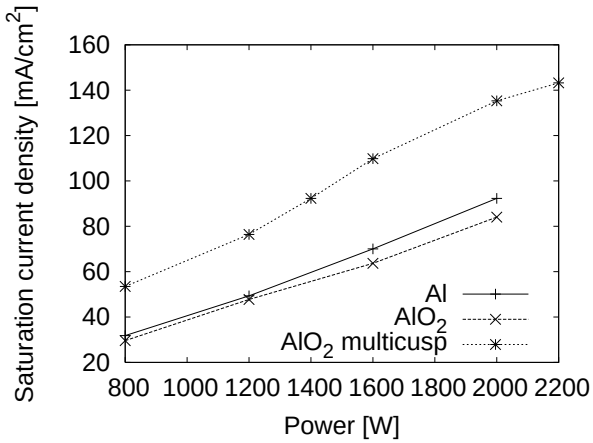

Figure 7: Extracted saturation ion current densities plotted as a function of power at pressure of 1.3 Pa.

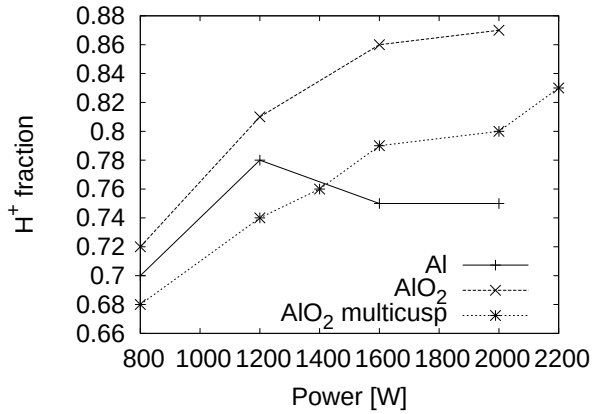

Figure 8: H^+ fraction plotted as a function of power at pressure of 1.3 Pa.

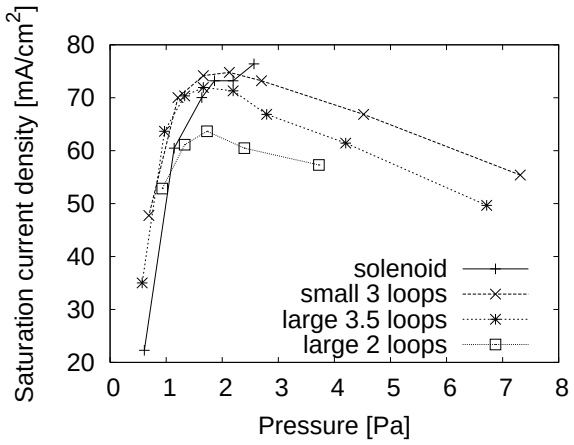

Figure 9: Saturation current versus pressure with different antennas at 1000 W of rf power.